The $PrAlO_3$−Pr_2O_3 Eutectic, its Microstructure, Instability, and Luminescent Properties

Dorota A. Pawlak,*,† Katarzyna Kolodziejak,† Ryszard Diduszko,† Krzysztof Rozniatowski,‡ Marcin Kaczkan,§ Michal Malinowski,§ Jaroslaw Kisielewski,† and Tadeusz Lukasiewicz†

Institute of Electronic Materials Technology, ul. Wolczynska 133, 01-919 Warsaw, Poland, Materials Science Department, Warsaw University of Technology, ul. Wołoska 141, 02-507 Warsaw, Poland, and Institute of Microelectronics and Optoelectronics, Warsaw University of Technology, ul. Koszykowa 75, 00-662 Warsaw, Poland

Received December 18, 2006. Revised Manuscript Received March 7, 2007

The praseodymium-aluminum perovskite−praseodymium oxide, $PrAlO_3$−Pr_2O_3, eutectic has been studied. The growth of the eutectic by the micro-pulling down method is presented. The $PrAlO_3$−Pr_2O_3 is not air-stable. The cause of the eutectic instability is the instability of the Pr_2O_3 phase. When exposed to air, the Pr_2O_3 phase changes into a new compound having a hexagonal unit cell with the lattice parameters $a = b = 6.455(1)$ Å, $c = 11.322(4)$ Å. The $PrAlO_3$−Pr_2O_3 eutectic grows with a regular complex microstructure. The luminescence spectra are presented for both the eutectic and the new phase generated by exposing the eutectic to air.

Introduction

Metal−metal eutectics have been studied for many years because of their excellent mechanical properties. Recently, oxide−oxide eutectics have also been studied for their excellent flexural strength and creep resistance at high temperature.[1−3] Experimental data for oxide−oxide eutectics or hybrid eutectics as metal−oxide, semiconductor−oxide are still very limited. Oxide−oxide eutectics were recently studied as optical materials[4,5] and proposed as materials that could act as photonic crystals.[6,7] Depending on different factors, such as the entropy of melting of both phases, eutectics can form different microstructures and nanostructures, classified by Hunt and Jackson as nonfaceted−nonfaceted, nonfaceted−faceted, and faceted−faceted.[8] The eutectic microstructure can exhibit many geometrical forms. It can be regular−lammelar, regular−fibrous, irregular, complex regular, quasiregular, broken−lamellar, spiral, or globular. The most interesting from the point of view of photonic crystals would be microstructures with regular shapes, i.e., lamellar and fibrous shapes, whereas for metamaterials[9,10] applications, other possible shapes would be also of interest, e.g., percolated structures for giant dielectric constant[11] or spiral for chiral metamaterials. A globular shape might also find application in invisible materials[12] or in plasmon tunable materials if the structure would be metallodielectric.[13]

In this paper, a newly manufactured eutectic compound is presented. It is $PrAlO_3$−Pr_2O_3 eutectic. The first results on the microstructure, the instability in an air atmosphere, and the luminescence properties of this eutectic are described in this paper. For a mixture of Al_2O_3 and Pr_2O_3 compounds, there are two possible kinds of eutectic structures: (1) $PrAlO_3$−$PrAl_{11}O_{18}$ eutectic at 1800 °C with composition 20.7% Pr_2O_3 and 79.3% Al_2O_3;[14] and (2) $PrAlO_3$−Pr_2O_3 eutectic at 1819 °C with composition 75% Pr_2O_3 and 25% Al_2O_3.[15] The first of these compositions has been studied elsewhere. In this paper, we report the growth of a eutectic with the second composition.

The investigated eutectic is interesting from the point of view of both its constituent compounds (i.e., $PrAlO_3$ and Pr_2O_3). Little is known about the praseodymium oxide because of its instability in air and its very high melting point. Praseodymium−aluminum perovskite is a very interesting material because of its phase transitions. $PrAlO_3$ undergoes three phase transitions,[16−18] which can be described as *C*2/*m*

* Corresponding author. E-mail: Dorota.Pawlak@itme.edu.pl. Tel: 48 22 8349949.
† Institute of Electronic Materials Technology.
‡ Materials Science Department, Warsaw University of Technology.
§ Institute of Microelectronics and Optoelectronics, Warsaw University of Technology.

(1) Waku, Y.; Nakagawa, N.; Wakamoto, T.; Ohtsubo, H.; Shimizu, K.; Kohtoku, Y. *Nature* **1997**, *389*, 49.
(2) Lee, J. H.; Yoshikawa, A.; Kaiden, H.; Lebbou, K.; Fukuda, T.; Yoon, D. H.; Waku, Y. *J. Cryst. Growth* **2001**, *231*, 179.
(3) Llorca, J.; Orera, V. M. *Prog. Mater. Sci.* **2006**, *51*, 711.
(4) Merino, R. I. *Phys. Rev. B* **1997**, *56*, 10907.
(5) Orera, V. M. *Appl. Phys. Lett.* **1997**, *71*, 2746.
(6) Pawlak, D. A.; Lerondel, G.; Dmytruk, I.; Kagamitani, Y.; Durbin, S.; Fukuda, T. *J. Appl. Phys.* **2002**, *91*, 9731.
(7) Merino, R. I.; Pena, J. I.; Larrea, A.; de la Fuente, G. F.; Orera, V. M. *Recent Res. Dev. Mater. Sci.* **2003**, *4*, 1.
(8) Hunt, J. D.; Jackson, K. A. *Trans. AIME* **1966**, *236*, 843.
(9) Pendry, J. B. *Phys. Rev. Lett.* **2000**, *85*, 3966.
(10) Shelby, R.; Smith, D. R.; Schultz, S. *Science* **2001**, *292*, 77.
(11) Pecharroman, C.; Esteban-Betegon, F.; Bartolome, J. F.; Lopez-Esteban, S.; Moya, J. S. *Adv. Mater.* **2001**, *13*, 1541.
(12) Garcia de Abajo, F. J.; Gomez-Santos, G.; Blanco, L. A.; Borisov, A. G.; Shabanov, S. V. *Phys. Rev. Lett.* **2005**, *95*, 067403.
(13) Riikonen, S.; Romero, I.; Garcia de Abajo, F. J. *Phys. Rev. B* **2005**, *71*, 235104.
(14) Pawlak, D. A.; Kolodziejak, K.; Diduszko, R.; Kaczkan, M.; Malinowski, M.; Piersa, M.; Lukasiewicz T. $PrAlO_3$−$PrAl_{11}O_{18}$ eutectic−its microstructure and spectroscopic properties. *Cryst. Growth Des.* **2007**, submitted.
(15) Mizuno, M.; Yamada, T.; Noguchi, T. *Nagoya Kogyo Gijutsu Shikensho Hokoku* **1978**, *27*, 45.

10.1021/cm063000s CCC: $37.00
Published on Web 04/05/2007

$\xrightarrow{150K}$ *Imma* $\xrightarrow{205K}$ *R*3*c* $\xrightarrow{1650K(1770K)}$ $Pm\bar{3}m$.[19−21] The Brillouin scattering measurements reveal a fourth transition at 150 K to *I*4/*mcm* that could not been found by X-ray diffraction.[22−24] The phase transitions are reflected in the physical properties of this material at different temperatures. The $PrAlO_3$ crystal seems to have an antiferroelastic nature.[22,23] The existence of ferroelastic microdomains and microtwin domains has been reported.[25,26] Also, it seems to exhibit interesting emission properties. The broad emission band of the as-grown $PrAlO_3$ crystal covers the visible spectrum,[26] which suggests potential application as a tunable laser in the whole visible region. Unfortunately at this stage, the emission seems rather weak. One of the ways to enhance the emission, apart from diluting the amount of praseodymium ion, would be preparing the $PrAlO_3$ crystal in the form of a microstructured or nanostructured material as, for example, the eutectic material in this paper.

Experimental Section

Crystal Growth. The micro-pulling down method was invented in Japan originally for growth of single-crystal fibers.[27,28] The growth of oxide−oxide eutectics for high-strength materials has already been presented by this method.[29,30] The micro-pulling down method utilizes a crucible with a die at the bottom in which there is centrally placed nozzle. The raw materials are melted in the crucible; the melt that exudes from the nozzle is touched with the seed crystal, and the crystal is pulled down. The details of the thermal system we used for micro-pulling down, as well as the growth conditions, are described elsewhere.[31] The crystals were seeded grown with a $YAlO_3$ single crystal. High-purity oxide powders (99.995%), Al_2O_3, and Pr_6O_{11} were used as starting materials. The oxides were mixed with ethanol in an alumina mortar and then dried.

X-ray Diffraction. X-ray powder diffraction measurements were performed on the as-grown, annealed, and demolished samples using a Siemens D500 diffractometer equipped with semiconductor Si:Li detector and $K_\alpha Cu$ radiation. The powder diffraction pattern was measured in a $\theta/2\theta$ scanning mode with a step of 0.02° and counting time of 10 s/step. The experimental data were analyzed by the Rietveld refinement using the DBWS-9807 program package of Young.[32] The orientation of the eutectic was examined using a four-circle KUMA-diffraction KM4 diffractometer and $K_\alpha Cu$ radiation.

Quantitative Analysis of the Microstructure. All the geometrical parameters were calculated from the scanning electron microscope images by the MICROMETER program.[33]

Spectroscopic Measurements. Luminescence of the samples was excited by a cw Carl Zeiss ILA 120 argon laser. The visible emission signal from the sample was dispersed by CVI DK 480 monochromator and detected by a cooled EMI C1034-02 GaAs photomultiplier. Data acquisition was performed using a computer-controlled Stanford SR 510 lock-in amplifier. All measurements were performed at room temperature.

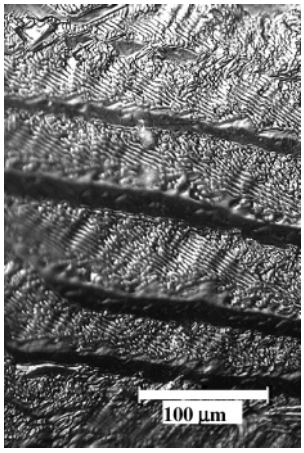

Figure 1. Optical microscopy image of the surface of the crystal, revealing its complex regular microstructure.

Results and Discussion

In this work, the $PrAlO_3-Pr_2O_3$ eutectic with composition of 75% Pr_2O_3 and 25% Al_2O_3 was grown by the micro-pulling down method with different pulling rates (p.r.): 0.15, 0.3, 0.45, 1, and 5 mm/min. The as-grown eutectic rods are black. This black coloration presumably arises from Pr^{4+} ions (the commonly used praseodymium oxide, Pr_6O_{11}, also has black coloration). Praseodymium can have two oxidation states, 3+ and 4+. The typical coloration of compounds containing Pr^{3+} ions is light green. To remove some of the Pr^{4+} ions, the samples of as-grown eutectics were annealed in a vacuum. Annealing changes the sample color from black to dark green.

Eutectic Microstructure. The eutectic microstructure is evident even in an optical microscope image of the surface (parallel to the growth direction) of the eutectic rod, Figure 1. It can be seen from this photo that there are long precipitates, and next to them, a lamellar-like eutectic microstructure is clearly visible. From the SEM images, the $PrAlO_3-Pr_2O_3$ eutectic microstructure has been identified as a complex regular structure, Figure 2. In all cases, $PrAlO_3$ is represented on the SEM images by the black color, and

(16) Howard, C. J.; Stokes, H. *Acta Crystallogr., Sect. B* **1998**, *54*, 782.
(17) Cohen, E.; Risberg, L. A.; Nordland, W. A.; Burbank, R. D.; Sherwood, R. C.; Van Uitert, L. G. *Phys. Rev.* **1969**, *186*, 476.
(18) Burbank, R. D. *J. Appl. Cryst.* **1970**, *3*, 112.
(19) Moussa, S. M.; Kennedy, B. J.; Hunter, B. A.; Howard, C. J.; Vogt, T. *J. Phys. Condens. Matter* **2001**, *13*, L203.
(20) Howard, C. J.; Kennedy, B. J.; Chakoumakos, B. C. *J. Phys. Condens. Matter* **2000**, *12*, 349.
(21) Carpenter, M. A.; Howard, C. J.; Kennedy, B. J.; Knight, K. S. *Phys. Rev. B* **2005**, *72*, 024118.
(22) Watanabe, S.; Hidaka, M.; Yoshizawa, H.; Wanklyn, B. M. *Phys. Status Solidi B* **2006**, *243*, 424.
(23) Fleury, P. A.; Lazay, P. D.; Van Uitert, L. G. *Phys. Rev. Lett.* **1974**, *33*, 492.
(24) Harley, R. T. *J. Phys. C: Solid State Phys.* **1977**, *10*, L205.
(25) Kim, C. H.; Cho, S. Y.; Kim, I. T.; Cho, W. J.; Hong, K. S. *Mater. Res. Bull.* **2001**, *36*, 1561.
(26) Pawlak, D. A.; Lukasiewicz, T.; Carpenter, M.; Malinowski, M.; Diduszko, R.; Kisielewski, J. *J. Cryst. Growth* **2005**, *282*, 260.
(27) Yoon, D. H.; Yonenaga, I.; Ohnishi, N.; Fukuda, T. *J. Cryst. Growth* **1994**, *142*, 339.
(28) Rudolf, P.; Fukuda, T. *Cryst. Res. Technol.* **1999**, *34*, 3.
(29) Lee, J. H.; Yoshikawa, A.; Durbin, S. D.; Yoon, D. H.; Fukuda, T.; Waku, Y. *J. Cryst. Growth* **2001**, *222*, 791.
(30) Lee, J. H.; Yoshikawa, A.; Kaiden, H.; Lebbou, K.; Fukuda, T.; Yoon, D. H.; Waku, Y. *J. Cryst. Growth* **2001**, *231*, 179.
(31) Kolodziejak, K.; Turczynski, S.; Diduszko, R.; Klimek, L.; Pawlak, D. A. *Optoelectron. Rev.* **2006**, *14*, 203.
(32) Young, R. A. *J. Appl. Cryst.* **1995**, *28*, 366.
(33) Wejrzanowski, T.; Bucki J. J. MICROMETER 0.99b, Computer Program for Image Analysis. MSc Thesis, Warsaw University of Technology, Warsaw, Poland, 2000.

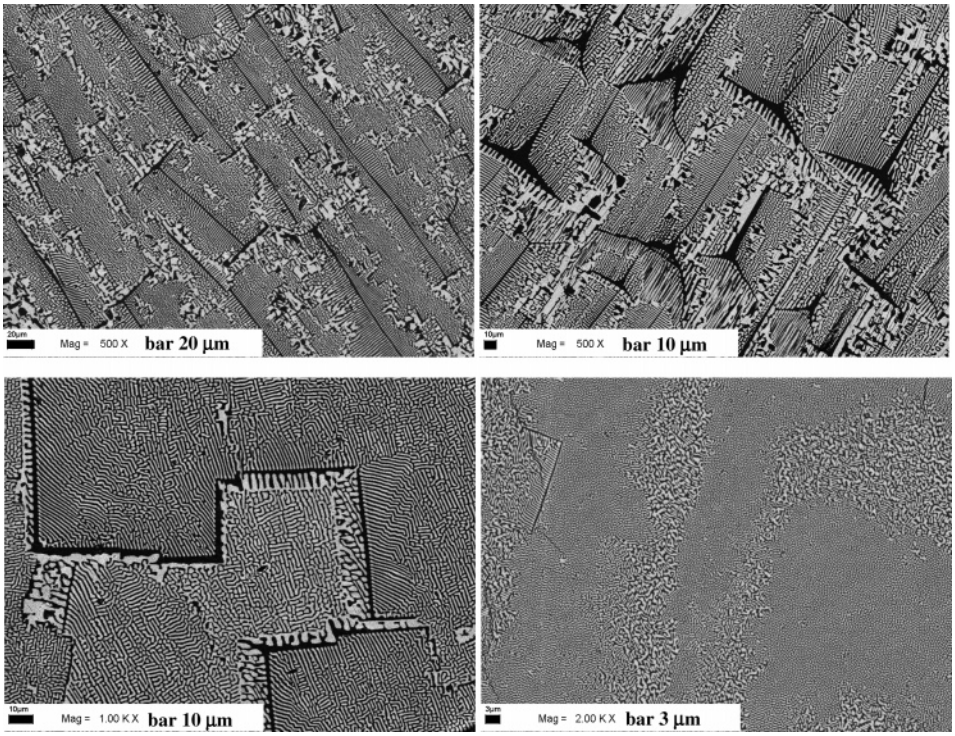

Figure 2. SEM images of the regular complex structure of $PrAlO_3-Pr_2O_3$ eutectic, cross-section.

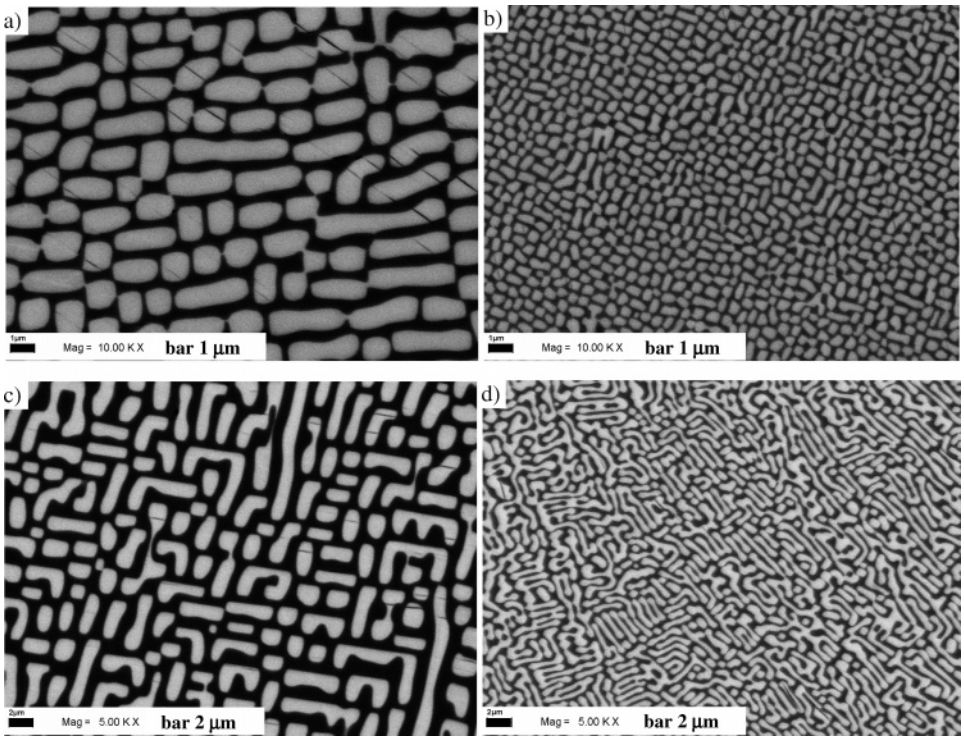

Figure 3. Two typical kinds of eutectic microstructure observed in the cross-section of $PrAlO_3-Pr_2O_3$ eutectic: (a, c) grown with p.r. = 0.45 mm/min, (b, d) grown with p.r. = 5 mm/min (black color, $PrAlO_3$ phase; white color, Pr_2O_3 phase).

Pr_2O_3 is represented by the white color, as confirmed by energy dispersive spectrometry (EDS). In the complex regular structures, one of the phases is a faceted crystal, and the eutectic follows the growth of this crystal. As a result, $PrAlO_3-Pr_2O_3$ eutectic grains grow with boundaries described by the skeletal structure[34] of the faceted crystal, in this case, the $PrAlO_3$ crystal (black-colored, bigger linelike precipitates, evident in Figure 2). In between the skeletal structure of the $PrAlO_3$ crystal, two types of eutectic microstructure have been found, Figure 3. In cross-section, one of them appears as a bricklike structure (images a and b of Figure 3) and the other a percolated structure (images

(34) Bagheri, S. D.; Rutter, J. W. *Mater. Sci. Technol.* **1997**, *13*, 541.

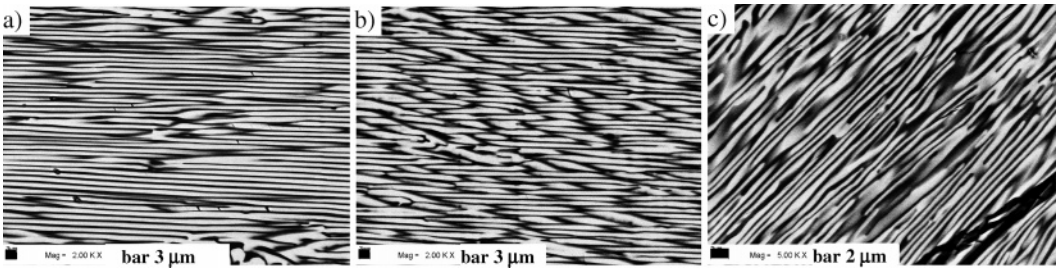

Figure 4. Longitudinal section of the eutectic, presenting the eutectic microstructure parallel to the growth direction (black color, $PrAlO_3$ phase; white color, Pr_2O_3 phase).

Table 1. Quantitative Analysis of Mean Size of the $PrAlO_3-Pr_2O_3$ Eutectic Microstructure[a]

kind of microstructure	p.r. (mm/min)	$<V_V>$	$<S_V>$ (μm^{-1})	$<d_2>$ (μm)	$<d_{min}>$ (μm)	$<d_{max}>$ (μm)
bricklike	0.45	0.54	1.6 (0.55)	1.4 (0.20)	1.0 (0.14)	2.0 (0.47)
bricklike	5	0.46	5.6 (0.47)	0.5 (0.25)	0.4 (0.28)	0.7 (0.51)
percolated	0.45	0.46	1.5 (0.47)	1.9 (0.26)	1.5 (0.35)	2.8 (0.41)
percolated	5	0.53	3.3 (2.05)	1.3 (0.78)	1.2 (0.96)	2.4 (0.96)

[a] p.r. = crystal pulling rate, $<V_V>$ = volume fraction of Pr_2O_3 phase, $<S_V>$ = specific surface of phase boundaries, $<d_2>$ = mean equivalent diameter of the Pr_2O_3 "particle", $<d_{min}>$ = mean minimal chord intercept of the Pr_2O_3 "particle", $<d_{max}>$ = mean maximal chord intercept of the Pr_2O_3 "particle". The numbers in the brackets indicate coefficient of variation, CV, where $CV(x) = SD(x)/<x>$. When CV is close to zero, all the parameters in the investigated area are similar.

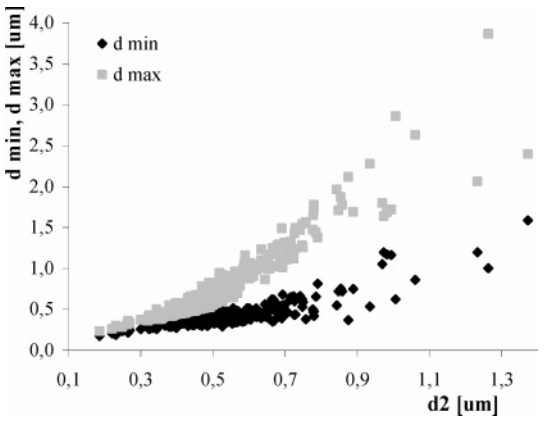

Figure 5. Relation between minimal/maximal intercept chord and the size of cross-section as a function of equivalent diameter (bricklike structure, p.r. = 5 mm/min).

c and d of Figure 3). In the longitudinal section, the eutectic structure is lammelar, with individual lammelas being broken and interconnected with each other (Figure 4a−c). The summary of the quantitative analysis of the eutectic microstructure is given in Table. 1.

The bricklike structure can be understood in three dimensions as plates, which are elongated in the growth direction and appear as bricks in cross-section. In all the areas where the bricklike structure is found, the growth of a "brick" is realized mainly by its unidirectional elongation. It can be observed that for all investigated SEM images with this kind of microstructure, the maximal chord intercept, d_{max} ("length" of the particle section), as a function of the cross-section equivalent diameter, d_2 ("size" of particle section), grows much faster than minimal chord intercept, d_{min} ("thickness" of particle section). An example of this behavior is shown in Figure 5 (in the bricklike structure, the bigger brick particles are significantly elongated).

The shape of the "particles" in the eutectic microstructure can be described by two shape factors a and b. The shape factor a describes the elongation of the particle cross-section and b represents the development of boundaries between the particle (the Pr_2O_3 phase) and the matrix (the $PrAlO_3$ phase); $a = (d_{max})/d_2$, $b = p/(\pi d_2)$, where p stands for particle perimeter. From Figure 6a, it can be seen that for the bricklike structure, the elongation of the particle cross-section (as a function of particle size) increases similarly to the development of boundaries between the particles and the matrix. For the percolated-like structure, the boundary lengths increase significantly faster than the elongation of particles, Figure 6b. The volume fraction of the $PrAlO_3$ phase, calculated on the basis of the surface fraction, differs in the samples from 0.46 to 0.54. The bricklike structure has bigger specific surface of phase boundaries ($S_v = 1.6$ and 5.6 μm^{-1}), and smaller equivalent diameter ($d_2 = 1.4$ and 0.5 μm) than the percolated structure ($S_v = 1.5$ and 3.3 μm^{-1}, $d_2 = 1.9$ and 1.3 μm), see Table 1. There also exists a tendency for the mean perimeter of the bricklike particles to decrease with increasing pulling rate, whereas the mean perimeter of the cross-section of the percolated structure particles increases with the pulling rate. It is not indicated in the table because of a very high standard deviation for the perimeter.

Also, a typical lammelar pattern is often observed next to the skeletal structure of $PrAlO_3$ phase (bigger precipitates of this phase), Figure 7, which after some distance changes into a eutectic pattern that is typical for this structure, Figure 3.

The $PrAlO_3-Pr_2O_3$ eutectic has been grown with different pulling rates. The smallest regions of structuring were observed in crystals produced by pulling at 5 mm/min, Figures 3 and 7. In the case of the lammelar structure, the mean width of the Pr_2O_3 phase and the $PrAlO_3$ phase is 1.19 and 0.89 μm (for the eutectic grown with p.r. = 0.45 mm/min, Figure 7b) and 0.36 and 0.27 μm (for the eutectic grown with p.r. = 5 mm/min, Figure 7c), respectively.

Eutectic Instability in Air. The eutectic $PrAlO_3-Pr_2O_3$ is not air−stable. After ca. 1.5 weeks of exposure to air, it turns into a fine yellow powder, as shown in Figure 8. The yellow powder consists of $PrAlO_3$ and another unidentified crystalline phase. The cause of the instability of the eutectic is the instability of Pr_2O_3 phase. This air-instability of the Pr_2O_3 phase has been previously reported in the literature[35]

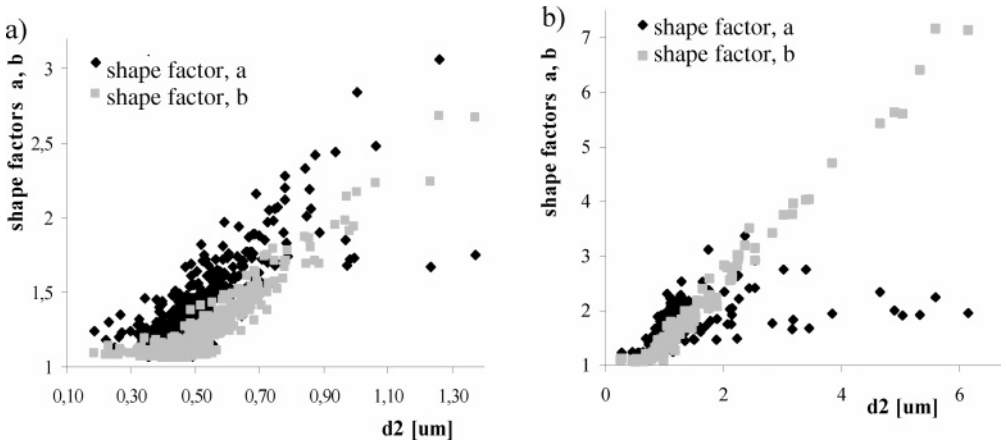

Figure 6. Shape factors of individual cross-sections as a function of its size, estimated by equivalent diameter: (a) bricklike structure, p.r. = 5 mm/min, (b) percolated structure, p.r. = 5 mm/min.

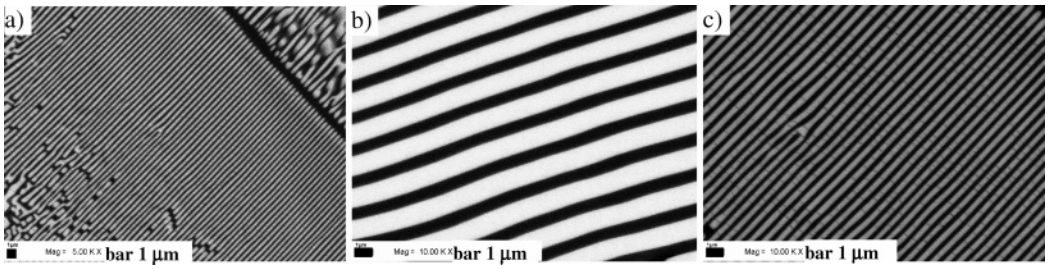

Figure 7. Lamellar eutectic microstructure existing at bigger precipitates of the $PrAlO_3$ phase: (a) general view, (b) eutectic grown with p.r. = 0.45 mm/min, (c) eutectic grown with p.r. = 5 mm/min (black color, $PrAlO_3$ phase; white color, Pr_2O_3 phase).

Figure 8. Degradation of the black $PrAlO_3-Pr_2O_3$ eutectic rod into a yellow fine powder, after ca. 1 week of exposure to air.

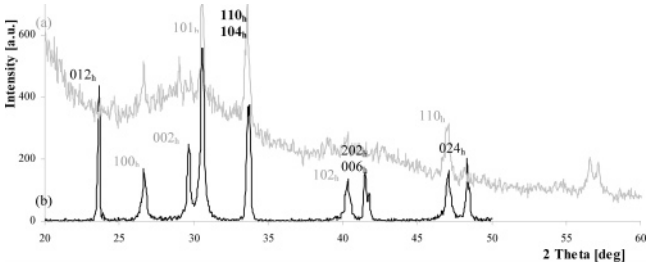

Figure 9. X-ray diffraction pattern of as-grown $PrAlO_3-Pr_2O_3$ eutectic: (a) single-crystal measurement, gray line; (b) powder measurement, black line. The black letters indicate the peaks from $PrAlO_3$ phase and the gray letters indicate peaks from Pr_2O_3 phase.

and probably explains the lack of available data for this compound. Another reason for a lack of literature data is the high melting point of Pr_2O_3 (2290 °C). In the eutectic composition, we obtain this phase only at 1819 °C. Storing the eutectic crystal in a nitrogen atmosphere prevents degradation.

X-ray powder diffraction confirms the presence of only $PrAlO_3$ and Pr_2O_3 phases in the as-grown $PrAlO_3-Pr_2O_3$ eutectic, Figure 9 b. Both compounds crystallize in the rhombohedric system. $PrAlO_3$ crystallizes in the $R(O)$ space group with the lattice constants $a = 5.332$ Å, $c = 12.97$ Å (hexagonal notation).[36] Pr_2O_3 crystallizes in the $P\bar{3}m1$ space group with lattice constants $a = 3.8589$ Å, $c = 6.0131$ Å (hexagonal notation).[37] Single-crystal X-ray diffraction from the plane of the eutectic rod perpendicular to the growth direction reveals that the $PrAlO_3$ crystal grows in the $<101>_r$ direction ($<110>_h$), Figure 10 a. The Pr_2O_3 phase does not show any specific crystallographic direction of growth.

Powder diffraction of the yellow powder formed from the degraded eutectic after ca. 1.5 week reveals that the $PrAlO_3$ phase is unchanged, whereas the Pr_2O_3 phase changes into a new compound (probably an oxide with different stoichiometry), which crystallizes in the hexagonal system with lattice constants $a = b = 6.455(1)$, $c = 11.322(4)$ Å and unit-cell volume 408.55 Å,[3] Figure 10 b. Using the TREOR90 program[38] all the signals have been indexed for such a unit cell, and the results are listed in Table 2. Although there are many different praseodymium oxides described in

(35) Osten, H. J.; Bugiel, E.; Dabrowski, J.; Fissel, A.; Guminskaya, T.; Liu, J. P; Müssig, H. J.; Zaumseil, P. *Epitaxial Prasedymium Oxide: A New High-K Dielectric*; Presented at the International Workshop on Gate Insulators, Tokyo, Nov 2001.

(36) Mizuno, M. et al., *Yogyo Kyokaishi − J. Ceram. Assoc. Jpn.* **1977**, *85*, 24.

(37) Greis, O.; Ziel, R.; Breidenstein, B.; Haase, A.; Petzel, T. *J. Alloys Compd.* **1994**, *216*, 255.

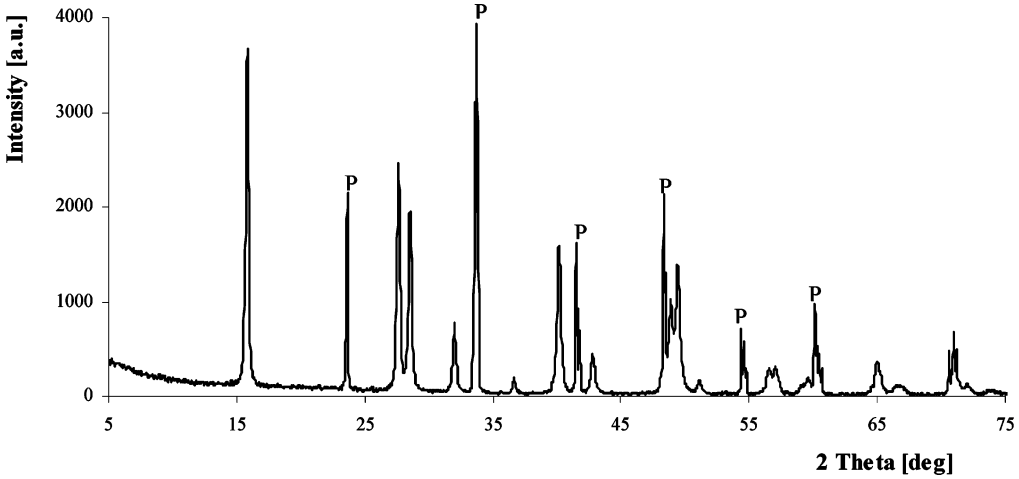

Figure 10. Powder X-ray diffraction pattern of the yellow powder—the rest of the $PrAlO_3-Pr_2O_3$ eutectic after ca. 1.5 week of exposure to air. The letter "P" indicates peaks with their origin from the $PrAlO_3$ phase.

Table 2. XRD Data for the Yellow Powder Derived from the Pr_2O_3 Phase of the $PrAlO_3-Pr_2O_3$ Eutectic after ca. 1.5 Weeks in Air

hkl	2θ **obsd**	2θ **calcd**
100	15.855	15.853
110	27.644	27.638
103	28.540	28.536
112		31.918
200	32.006	32.020
113	36.652	36.635
203	40.144	40.145
210	42.782	42.798
300	48.881	48.876
213	49.450	49.435
106	51.100	51.084
116	56.514	56.488
220	57.085	57.072
107		59.493
222	59.599	59.569
310		59.632
313	64.958	65.033
224	66.758	66.720
207		66.825
306	71.193	71.101
403	72.002	72.062
320	73.957	73.899
009	75.542	75.583
109	77.809	77.823
226		77.890
323	78.802	78.820
412	80.550	80.550

the literature, no data could be found for an oxide with similar unit cell. The ratio of the volume of $PrAlO_3$ phase to the volume of the new phase in the yellow powder is on the same order of magnitude as the ratio of $PrAlO_3$ and Pr_2O_3 volumes in the eutectic crystal. Consequently it is uncertain whether the new phase is a new version of praseodymium oxide, or if the new compound contains also some aluminum ions: both options seem to be possible. In the first case, it is known that oxide of praseodymium containing only Pr^{3+} ions is unstable (the air-stable oxide is Pr_6O_{11}). So it is normal that in air, Pr_2O_3 will oxidize to give an oxide closer to this mixed one. But the surprising feature here is the light-yellow color of the powder, which is also air-stable at room temperature. When annealed in air, it becomes dark brown (we remind the reader that Pr_6O_{11} is black because of the presence of Pr^{4+} ions). The other possibility is that, during the growth of the eutectic, some of aluminum ions "dissolve" in the Pr_2O_3 phase in a disordered manner, although this amount is sufficiently small that the structure of Pr_2O_3 is not influenced. Exposure of this Pr_2O_3 to air with some dissolved aluminum might cause transformation to a compound partially doped with aluminum. This second hypothesis is supported by XPS results[39] showing one big Al 2p peak at an energy characteristic for $PrAlO_3$[40] and one small peak at energies close to binding energies of Al 2p in Al_2O_3 for the as grown $PrAlO_3-Pr_2O_3$ eutectic. In the case of the yellow powder, the Al 2p peak at the binding energies characteristic for Al_2O_3 is strongly increased.

In Figure 11 the room-temperature emission spectra of the as-grown $PrAlO_3-Pr_2O_3$ eutectic (black line) is presented and compared with the emission spectrum of a $PrAlO_3$ crystal (gray line).[26] The presented eutectic is grown with the pulling rate 5 mm/min. In the inset, the comparison of the intensities of the spectra of eutectics grown with different pulling rates, as well as the $PrAlO_3$ crystal, are presented: (a) first from the top, as-grown $PrAlO_3-Pr_2O_3$ eutectic grown with p.r. = 5 mm/min (black line); (b) second from top, as-grown $PrAlO_3-Pr_2O_3$ eutectic grown with p.r. = 0.45 mm/min (dark gray line); and (c) third from the top, $PrAlO_3$ crystal (light gray line). As seen in the inset, the emission of the $PrAlO_3-Pr_2O_3$ eutectic is significantly more intense than the emission from $PrAlO_3$ crystal.[26] In addition, the intensity of emission of the eutectic grown with a 5 mm/min pulling rate is also higher than emission of the eutectic grown with a 0.45 mm/min pulling rate. It can be seen that the emission spectrum of the $PrAlO_3-Pr_2O_3$ eutectic is a superposition of $PrAlO_3$ and Pr_2O_3 spectra. The emission peaks in Figure 11 were assigned to emission transitions coming from the $PrAlO_3$ phase (gray colored *, Table 3) and the Pr_2O_3 phase (black colored ●, Table. 3). The assignment of emission peaks of

(38) Werner, P. E. *TREOR90*; part of *WINPLOTR*: Roisnel, T.; Rodríguez-Carvajal, J. *WinPLOTR: A Windows Tool for Powder Diffraction Patterns Analysis*; Materials Science Forum, Proceedings of the Seventh European Powder Diffraction Conference (EPDIC 7), Barcelona, May 20−23, 2000; Delhez, R., Mittenmeijer E. J, Eds.; Trans Tech Publications: Aedermannsdorf, Switzerland, 2000, pp 118−123.

(39) Kruczek, M.; Talik, E.; Pawlak, D. A.; Kolodziejak, K.; Lukasiewicz, T. XPS study of $PrAlO_3$-$PrAl_{11}O_{18}$ and $PrAlO_3$-Pr_2O_3 eutectics *J. Alloys Compd.* **2007**, in press, doi:10.1016/j.jallcom.2006.08.361.

(40) Kruczek, M.; Talik, E.; Pawlak, D. A.; Lukasiewicz, T. *Opt. Appl.* **2005**, *35*, 347.

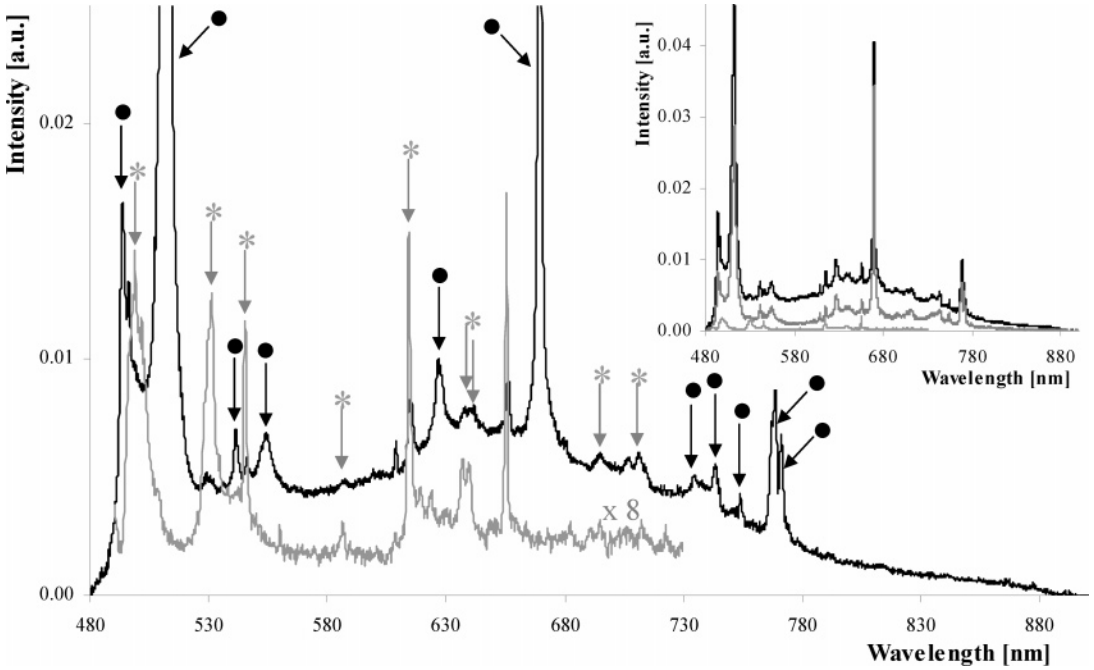

Figure 11. Emission spectra of as-grown (p.r. = 5 mm/min) $PrAlO_3-Pr_2O_3$ eutectic (black line) in comparison with emission spectra of $PrAlO_3$ crystal (gray line),[26] exc. 458 nm, argon laser. Inset: Comparison of the intensities of emission spectra of as-grown $PrAlO_3-Pr_2O_3$ eutectic grown with p.r. = 5 mm/min (black line), as-grown $PrAlO_3-Pr_2O_3$ eutectic grown with p.r. = 0.45 mm/min (dark gray line), and a $PrAlO_3$ crystal (light gray line), measured in the same experimental conditions. * stands for emission peaks from $PrAlO_3$ phase, ● stands for emission peaks from Pr_2O_3 phase.

Table 3. Assignment of the Observed Emission Transitions from $PrAlO_3$ and Pr_2O_3 Phase in $PrAlO_3-Pr_2O_3$ Eutectic Compared with $PrAlO_3$ Single-Crystal Emission Transitions at Room Temperature

	wavelength (nm)		
assigned transition	$PrAlO_3$ single crystal	$PrAlO_3$ in the eutectic	Pr_2O_3
$^3P_0 \rightarrow {}^3H_4$	499.0	499.0	494.0
	501.8		496.5
	509.0		512.6
$^3P_0 \rightarrow {}^3H_5$	531.3	531.2	
	545.3	546.3	541.7
	560.0		555.0
$^3P_0 \rightarrow {}^3H_6$	586.8	589.1	
	610.5	609.0	
$^1D_2 \rightarrow {}^3H_4$	614.3	615.5	627.7
$^3P_0 \rightarrow {}^3H_6$	619.5		
	624.0		627.7
	637.3	638.0	
	640.0	640.0	
$^3P_0 \rightarrow {}^3F_2$	655.3	656.1	669.5
$^3P_0 \rightarrow {}^3F_3$;			736.0
$^1D_2 \rightarrow {}^3H_5$			
$^3P_0 \rightarrow {}^3F_3$,4			743.7
$^3P_0 \rightarrow {}^3F_4$			754.1
			768.6
			771.3

Pr_2O_3 phase was on the basis of the energy levels of Pr^{3+} in Pr_2O_3 and energy levels and emission spectra of La_2O_3:Pr described in ref 41.[41] The assignment of the $PrAlO_3$ phase emission peaks was on the basis of the experimentally measured emission spectrum of the $PrAlO_3$ crystal[26] as well as the energy levels of $LaAlO_3$:Pr crystal, which is isostructural with $PrAlO_3$.[42,43] Measurements of decay times were unsuccessful because of low emission intensity and very short decay times. Hence, it was not possible on the basis of the fluorescence dynamics to clearly assign some peaks of the Pr_2O_3 phase to corresponding emission transitions (Table 3).

From Figure 11, it can be deduced that the emission of $PrAlO_3-Pr_2O_3$ eutectic is dominated by the Pr_2O_3 contribution. The eutectic was grown from the composition 75%Pr_2O_3 + 25%Al_2O_3, so there should be similar molar ratio of the Pr_2O_3 and $PrAlO_3$ phases. This could result in more intense emission from the Pr_2O_3 phase than from $PrAlO_3$ phase. The differences in the emission intensities of $PrAlO_3$ and Pr_2O_3 phases could also result from different absorption efficiencies of these phases at the excitation wavelength of 458 nm, or different quantum efficiencies of $^3P_0$ level. It could be also that the luminescence coming from $PrAlO_3$ gets significantly absorbed by the contiguous Pr_2O_3 phase on its way through the crystal.[4] Because of the high Pr^{3+} ion density in the lattice, the emission efficiency from the $^3P_0$ state is strongly related to mutual interactions between Pr^{3+} ions in the lattice. In Pr_2O_3, there are two praseodymium ions per molecule and there is one molecule of Pr_2O_3 in a unit cell of volume equal to 77.5 Å,[3] which gives 26×10^{21} atoms/cm^3.[44,45] In $PrAlO_3$, there is only one praseodymium ion per molecule but there are two molecules per unit cell (volume 106.5 Å^3), which gives 19×10^{21} atoms/cm^3.[46] Hence, drawing a sphere with a radius of 4.5 Å around an praseodymium ion in $PrAlO_3$, there are six neighboring praseodymium ions. In the case of Pr_2O_3, there are twelve praseodymium ions surrounding the considered ion. The number of nearest-neighbor Pr···Pr pairs in this sphere is six in $PrAlO_3$, with all distances equal to 3.762 Å, whereas there are twelve such Pr···Pr pairs in Pr_2O_3,

(41) Moune, O. K.; Faucher, M. D.; Jayasankar, C. K.; Lejus, A. M. *J. Luminesc.* **1999**, *85*, 59.
(42) Martin-Brunetiere, F.; *J. Phys. Paris* **1969**, *30*, 839.
(43) Pelletier-Allard, N.; Martin-Brunetiere, F.; *J. Phys. Paris* **1969**, *30*, 849.
(44) Greis, O.; Ziel, R.; Breidenstein, B.; Haase, A.; Petzel, T. *J. Alloys Compd.* **1994**, *216*, 255.
(45) Wolf, R.; Hoppe, R. *Z. Anorg. Allg. Chem.* **1985**, *529*, 61.
(46) Geller, S.; Bala, V. B. *Acta Crystallogr.* **1956**, *9*, 1019.

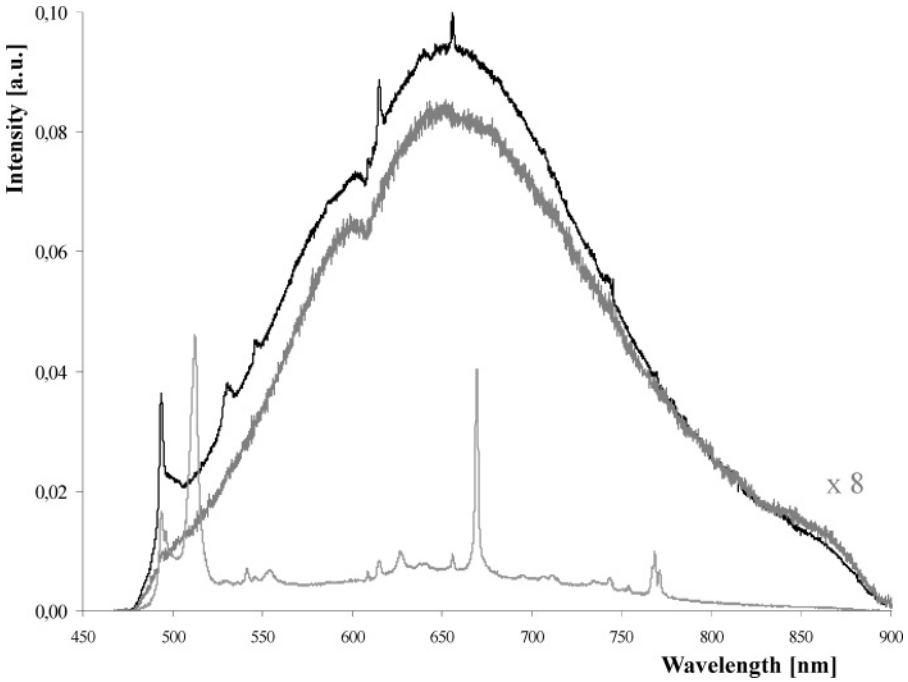

Figure 12. Black line, emission spectrum of the yellow powder into which the as-grown $PrAlO_3-Pr_2O_3$ eutectic degrades after ca. 1.5 week in air (exc. 458 nm, argon laser). Dark gray line, emission spectrum of the brown powder which is obtained by annealing the yellow powder in air. Light gray line, emission spectrum of $PrAlO_3-Pr_2O_3$ eutectic.[26]

with the following interatomic distances: 3×3.706, 3×3.778, 6×3.859 Å. This higher density of Pr ions could result in much higher concentration quenching in Pr_2O_3 compared to $PrAlO_3$. This poses the question: what is the reason for the much higher observed emission intensity of praseodymium in Pr_2O_3 compared to $PrAlO_3$?

We do not observe emission line energy shifts for a $PrAlO_3$ single crystal annealed in a reducing atmosphere compared to the crystalline $PrAlO_3$ phase in the $PrAlO_3-Pr_2O_3$ eutectic (Table 3). But significant differences in wavelength for the same emission transition are observed for Pr_2O_3 and $PrAlO_3$. For example, for $^3P_0 \rightarrow {}^3F_2$, it is ca. 13 nm (Table 3), which is in agreement with the energy level scheme. Because the splitting of the $^3F_2$ multiplet is very small, on the order of $50-120$ cm^{-1}, the peaks at 656.1 nm for the $PrAlO_3$ phase and 669.5 nm for the Pr_2O_3 phase must be related to unresolved $^3P_0 \rightarrow {}^3F_2$ transitions. In both compounds, it is the case that the praseodymium ion is not a dopant but rather a constituent ion, so there is a high density of active ions. This changes the crystal field in comparison to Pr-doped systems, which are relatively well-known.

The emission spectrum of the new compound (the yellow powder) into which degrades the $PrAlO_3-Pr_2O_3$ eutectic appears as a very broad band in the region from ca. 480 to 900 nm, Figure 12 (black line). The emission spectrum of the $PrAlO_3-Pr_2O_3$ eutectic is shown for comparison, Figure 12 (light gray line). On the broad band, some of the narrow emission peaks are still observed. When the yellow powder is pressed into a pellet and annealed in air, it changes color to dark brown. The emission from such a pellet is shown in Figure 12 (dark gray line). The emission band has the same shape as the emission from the yellow powder, but is less intense (probably due to higher absorption) and the narrow emission peaks are not present. It should be underlined that although the crystalline $PrAlO_3-Pr_2O_3$ eutectic has black coloration, which would suggest the presence of Pr^{4+} ions in addition to Pr^{3+} ions, the broad emission band that has been observed for a $PrAlO_3$ as-grown single crystal has not been observed for the crystalline eutectic. However, in absorption, a very wide absorption band between 300 and 1200 nm is observed, which can be connected with the presence of Pr^{4+} ions.[47] It remains unclear why, in the presence of air, the black colored crystalline $PrAlO_3-Pr_2O_3$ (containing probably Pr^{4+} and Pr^{3+} ions) eutectic changes into yellow powder (which would suggest no more Pr^{4+}).

Acknowledgment. The authors thank the Ministry of Scientific Research and Information Technology of Poland for support of this work (Grant 4 T11B 015 24). The authors acknowledge the Network of Excellence, METAMORPHOSE (500252). They also thank Dr Siân Howard (University of South Australia) for a critical reading of the first draft.

CM063000S

(47) Pawlak, D. A.; Frukacz, Z.; Mierczyk, Z.; Suchocki, A.; Zachara, J. *J. Alloys Compd.* **1998**, *275*, 361.